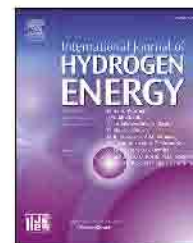


Available online at www.sciencedirect.com

ScienceDirect

journal homepage: www.elsevier.com/locate/he

Transmutations observed from pressure cycling palladium silver metals with deuterium gas

Gustave C. Fralick^a, Robert C. Hendricks^a, Wayne D. Jennings^b,
Theresa L. Benyo^{a,*}, Frederick W. VanKeuls^b, David L. Ellis^a,
Bruce M. Steinetz^a, Lawrence P. Forsley^c, Carl E. Sandifer II^a

^a National Aeronautics and Space Administration, Glenn Research Center, Cleveland, OH, 44135, USA

^b HX5, LLC, Cleveland, OH, 44135, USA

^c JWK Corporation, Annandale, VA, 22003, USA

HIGHLIGHTS

- Surface transmutations occurred in deuterium gas cycling experiments of PdAg tubes.
- Zn and Cr not present in PdAg before experiments were observed on PdAg afterwards.

ARTICLE INFO

Article history:

Received 30 June 2020

Received in revised form

30 August 2020

Accepted 31 August 2020

Available online xxx

Keywords:

Deuterium gas cycling

Palladium silver alloy

Elemental transmutations

Anomalous heating

ABSTRACT

Hydrogen, deuterium, and helium gases were separately cycled through a Johnson-Matthey purifier containing coiled palladium silver alloy tubing: Pd25Ag (75 wt% Pd and 25 wt% Ag). During the cycling of D₂ gas, evidence of anomalous heat production was observed. However, during the cycling of H₂ and He, very little (H₂) or no (He) unusual heat events were observed. After cycling the D₂ gas through the coiled tubing for several months, Pd25Ag samples showed an increase in Cu and Fe compared with the amounts in unexposed Pd25Ag. Chromium, manganese, and zinc were detected in gas-cycled Pd25Ag samples, whereas they were not detected in unexposed Pd25Ag samples. In particular, Zn was present in the gas-cycled Pd25Ag material in larger quantities than either Cr or Mn. Although a small amount of Cu was present in the Pd25Ag coil before the D₂ gas cycling, 7 times more was present after the cycling. Multiple material characterization techniques were used to obtain both pre-test and post-test elemental composition. The results indicate that novel post-test elements, primarily on the surface, were created by unknown nuclear mechanisms at low energy.

Published by Elsevier Ltd on behalf of Hydrogen Energy Publications LLC.

Introduction

Background

In 1989, Fralick and his NASA colleagues documented anomalous thermal behavior when performing tests with a

Johnson-Matthey (JM) hydrogen purifier loaded weeks prior with deuterium gas [1]. Fralick continued testing with the JM purifier cycling the deuterium gas at various pressures, temperatures and rate of compression, holding at constant conditions and expansion cycling-rates, noting each cycle produced a particular anomalous behavior. For example, anomalous heat was generated during one of the experiments

* Corresponding author.

E-mail address: Theresa.L.Benyo@nasa.gov (T.L. Benyo).

<https://doi.org/10.1016/j.ijhydene.2020.08.287>

0360-3199/Published by Elsevier Ltd on behalf of Hydrogen Energy Publications LLC.

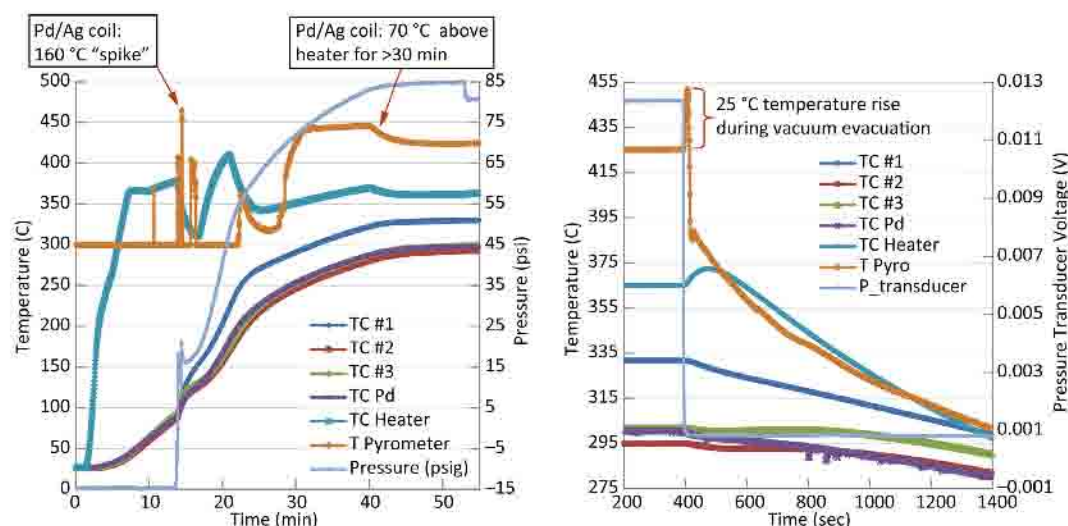


Fig. 1 Temperature data taken during one of the Pd25Ag JM experiment runs. Significant anomalous heat released during D₂ gas loading (left). Temperature spike of 25 °C during unloading of D₂ gas (right).

where the temperature of the Pd25Ag coil stayed at 70 °C above the heater setting for over 30 min after the loading of deuterium gas within the JM purifier as shown in the left side of Fig. 1. The right side of Fig. 1 shows the temperatures during the deuterium gas unloading and a 25 °C temperature rise which is not expected since the Joule-Thomson effect would induce cooling. Li et al. [2], Biberian and Armanet [3], and Liu et al. [4] have noted the same behavior with pumping deuterium gas in the presence of a Pd wire. Fig. 2 shows a photo of a JM hydrogen purifier opened up, exposing three concentric coils of Pd25Ag tubes. The inset X-ray image shows the internal plumbing that supplies initial "unpure hydrogen" and the small thin Pd25Ag coiled tubes supported by an inner stainless steel spring through which the resulting pure hydrogen flows. More detail on the hydrogen purification process can be found in Ref. [5–9]. After passing through the walls of these tubes, the gas is collected in a manifold (captured gas) from which the purified hydrogen (all isotopes) is extracted. During this early experiment, Fralick found the evidence of anomalous heat and enigmatic neutrons when the purifier was filled with D₂ at a temperature of 383 °C and a pressure of about 1380 kPa. The supply lines to the purifier had been pumped down, and the purifier was to be evacuated prior to running another background count. As the valve on the hydrogen purifier was cracked open to allow the gas to evacuate the pressure vessel, the temperature began to rise. He continued to open the valve slowly. By the time the valve was fully open (10 or 15 s), the temperature had increased to 400 °C before it began to decrease. During this time, the temperature control setting remained at 382 °C, and the temperature rise was much more rapid than was possible using the electric heater. The Joule-Thompson expansion should have cooled, not heated, the gas, further adding to the anomalous heating observed.

As is well documented by Storms [10], there are many researchers who have documented similar anomalous heat effects and the presence of anomalous material when cycling deuterium with Pd, Ti, and other base materials.

These researchers found interesting and similar effects when cycling deuterium gas through thin-film Pd [11,12] or Pd/CaO/Pd layers [13–15], such as producing heat [2,4,13,16] and/or transmutation of Pd into elements such as Cu. Takahashi et al. [17] offer a mechanism by which such transmutations within a PdD lattice may occur. Rather than use gas diffusion, Szpak et al. [18] independently observed surface transmutation producing unexpected elements during Pd/D/Li electrolytic co-deposition with external fields. All of these separate observations show that Pd and D appear to be the key ingredients in the observed transmutations.

Based on the more contemporary works and materials findings, it was decided to open the sealed hydrogen purifier originally tested in 1989 (JM-1) and examine if there were any anomalous material findings. Based on the JM-1 findings, a second Johnson-Matthey purifier (JM-2) was purchased and modified to incorporate better temperature sensing capabilities, to determine if the anomalous thermal results could be repeated and to determine if any anomalous material elements were found.

The objective of this paper is to document the novel findings that reveal materials transmutations of the Pd25Ag tubes

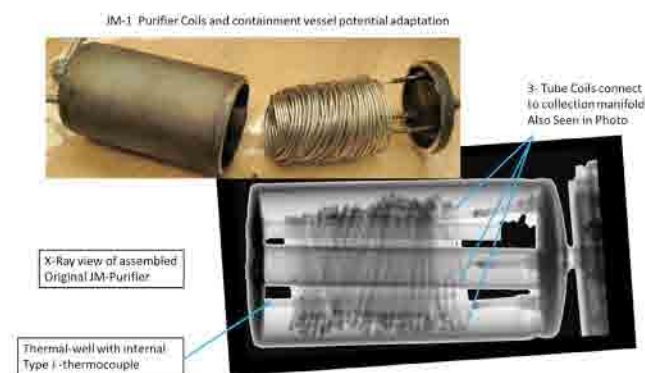


Fig. 2 JM-1: Pd25Ag coils and containment vessel.

within both JM hydrogen purifiers after each had been cycled, one at a time, with deuterium and hydrogen gases. Various analysis techniques were utilized to analyze the samples.

Experimental procedures and analytical methods

In normal operation of a JM purifier, three sets of coiled tubes with each Pd25Ag coil weighing ~17 g (~51 g total) are enclosed within a stainless steel (SS) container. The coiled tubes geometry was as follows. The length of each coil was 3.66 m. The outer coil's outside diameter was 49.9 mm, the central coil's outside diameter was 46.5 mm, and the inner coil's outside diameter was 42.9 mm. For each individual tube, the outside diameter was 1.59 mm with a tube thickness of 0.08 mm. An inner support SS spring was inside each tube. The SS spring's elemental concentrations were 74 wt% Fe, 18.5 wt% Cr, and 7.5 wt% Ni. The spring had a pitch of ~0.58 mm.

The chamber where the Pd25Ag coiled tubes are held is heated to prevent cracking of the tubes during gas cycling (where the H₂ or D₂ is diffused through the Pd25Ag tube walls). The manufacturer recommended an operating temperature >300 °C. During gas cycling, the internal chamber temperature was heated to 300–400 °C. These coiled tubes (nominally 1.5 mm in diameter) are connected to three collector ports. The SS container is filled through a separate single, much larger port. For these tests, both the coiled tubes and the container enclosure ports were connected through a common manifold by a three-way valve to either a pressure source or a large evacuated K-Bottle volume-sink at least 30 times the volume of the JM purifier and tubing. Thus, when the pressurized gas is "dumped" into the collection volume, the pressure in the JM purifier drops precipitously causing a large flux of the test gas through the walls of the Pd25Ag tubes.

Cycling involved allowing the system to equilibrate (usually overnight), wherein the unloaded deuterium gas that was "dumped" into the evacuated K-bottle sink was reabsorbed by the Pd25Ag tubing, essentially reloading the tubing with deuterium gas at ambient thermal conditions. This is an important point, as it is indicative that a portion of the deuterium gas will remain within the material lattice under most post-test conditions. With the valves reset, isolating the JM from the K-bottle, the system was then reheated to at least 300 °C, but no greater than 400 °C. This heating increased the pressure to nearly 0.7 MPa with differences made up from the deuterium bottle pressure source. A single run consisted of filling the JM purifier with a single gas (e.g., deuterium) and cycling that gas in/out of the system for a period of time (i.e., several months), which exposed the Pd25Ag tubes to different gases. In three separate runs, various test gases were cycled through the hydrogen purifier. In JM-1, deuterium and hydrogen were utilized separately, whereas in JM-2, primarily deuterium with a small number of runs using either hydrogen or helium gases were performed. (Note: helium was used as a control gas against which the hydrogen and deuterium runs could be compared for the thermal investigations). The gas purities were as follows: D₂ gas, 99.999% ultra-high purity; H₂ gas, 99.99% high purity; and He gas, 99.99% high purity.

In these first set of the most recent tests, JM-2 was filled with deuterium gas and cycled 141 times. Considering one

cycle was done per day and 5 cycles completed per week, the deuterium gas was cycled for a total of 28 weeks. Both the container and tubes were filled with the gas to determine the characteristics of rapid change in reaction and activity of the Pd25Ag. Subsequent cycling involved allowing the system to equilibrate (usually overnight) wherein the unloaded deuterium gas "dumped" into the evacuated K-bottle sink was reabsorbed by the Pd25Ag tubing.

Before changing gases, JM-2 including the K-bottle sink and lines were all evacuated. However, the gas bottle source was not involved in this evacuation. The JM-2 was valved-off, baked-out and evacuated several times to purge JM-2 of residual gases. Upon completion of purging the system, the K-bottle was again evacuated, valved-off, and JM-2 was loaded with H₂ gas to 0.7 MPa and heated to 300–400 °C with the same pre-test protocol as established by the D₂ testing.

After cycling H₂ ten times (for a total of 2 weeks), the system was purged following the protocol established and then JM-2 was cycled with helium twice for a total of 2 days.

Temperature at various locations within the JM-2 system was monitored during all 3 separate gas cycling activities. Temperature increases were noted during the loading and of all gases. Temperature decreases were noted during the unloading of all gases, however during the deuterium cycling, the temperature decrease was greater than the other 2 gases.

Analyses performed

To harvest the Pd25Ag tubes for subsequent analyses, the stainless steel pressure vessel needed to be cut open. It was decided to open the JM-1 SS pressure vessel with a silicon carbide (SiC) abrasive cutting wheel with no lubricants to prevent contamination of the internal elements and tubes with cutting fluids. In contrast, the JM-2 SS pressure vessel was opened with a tube cutter consisting of a martensitic SS cutting blade. After opening the cavity, tubes from JM-1 were harvested and analyzed using optical microscopy for macrostructural features. They were also analyzed for microstructural features with a scanning electron microscope with energy-dispersive X-ray spectroscopy (SEM/EDS), a surface analysis method, and time-of-flight secondary-ion-mass spectroscopy (TOF-SIMS). The tubes harvested from JM-2 were analyzed using SEM/EDS, inductively coupled plasma atomic emission spectroscopy (ICP-AES), a bulk sample analysis method, and TOF-SIMS. Tubes were also obtained from the manufacturer (Johnson-Matthey) to serve as baseline/control tubes for both ICP-AES and SEM/EDS materials analyses.

Results of analyses

Analysis of as-received Pd25Ag tubes: control

SEM/EDS microscopy

SEM/EDS determined that the material constituents of the control tubes from the manufacturer were ~27 wt% Ag and Pd (balance) at the surface where a variation from 25% is not out of the ordinary. Fig. 3(a) shows the SEM image of an as-received unexposed tube which is typical of this type of

tube. Notice that the surface has no marred areas and is relatively smooth. The grooved areas are most likely from the extrusion process when making the tubes. Fig. 3(b) shows the map sum spectrum of the area shown in Fig. 3(a) and contains at the surface, the expected ratio of Pd and Ag.

ICP-AES

Through ICP-AES, an unexposed Pd25Ag tube was found to contain 75 ± 0.1 wt% Pd and 25 ± 0.1 wt% Ag with trace amounts of Al, Cu, Fe, Mg, Na, Pt, and Si as listed in the "Control/Unexposed" column of Table 1.

Analysis of exposed Pd25Ag tubes: JM-1

Optical microscopy

On some of the JM-1 tubes, optical microscopy revealed unusual ringed structures as well as some pits and cracks. Fig. 4(a) shows three external rings each with an unusual center indication.

SEM/EDS microscopy

Upon greater magnification, the circular features revealed unusual three-dimensional structures, which appeared

Table 1 ICP-AES results of unexposed and exposed Pd25Ag.

Element	Pd25Ag Results			Units
	Control/Unexposed	Exposed	Δ	
Ag	25.0 ± 0.1	24.9 ± 0.1	-0.1	wt%
Pd	75.0 ± 0.1	75.1 ± 0.1	+0.1	wt%
Al	30 ± 10	30 ± 10	0	ppm
Cr	Not detected	2 ± 1	+2	ppm
Cu	20 ± 10	140 ± 10	+120	ppm
Fe	20 ± 5	40 ± 5	+20	ppm
Mg	1 ± 0.5	1 ± 0.5	0	ppm
Mn	Not detected	0.5 ± 0.2	+0.5	ppm
Na	2 ± 1	2 ± 1	0	ppm
Pt	105 ± 5	105 ± 5	0	ppm
Si	40 ± 10	30 ± 10	-10	ppm
Zn	Not detected	285 ± 5	+285	ppm

almost like craters or a bulls-eye inside an external ring of distressed material as shown in Fig. 4(b) (for reference, dashed lines are shown to highlight the ringed feature locations). The presence of these 3D structures indicate that localized heating (from the fact that they look molten) and shock propagation (as evidence of the rings around the feature) occurred during

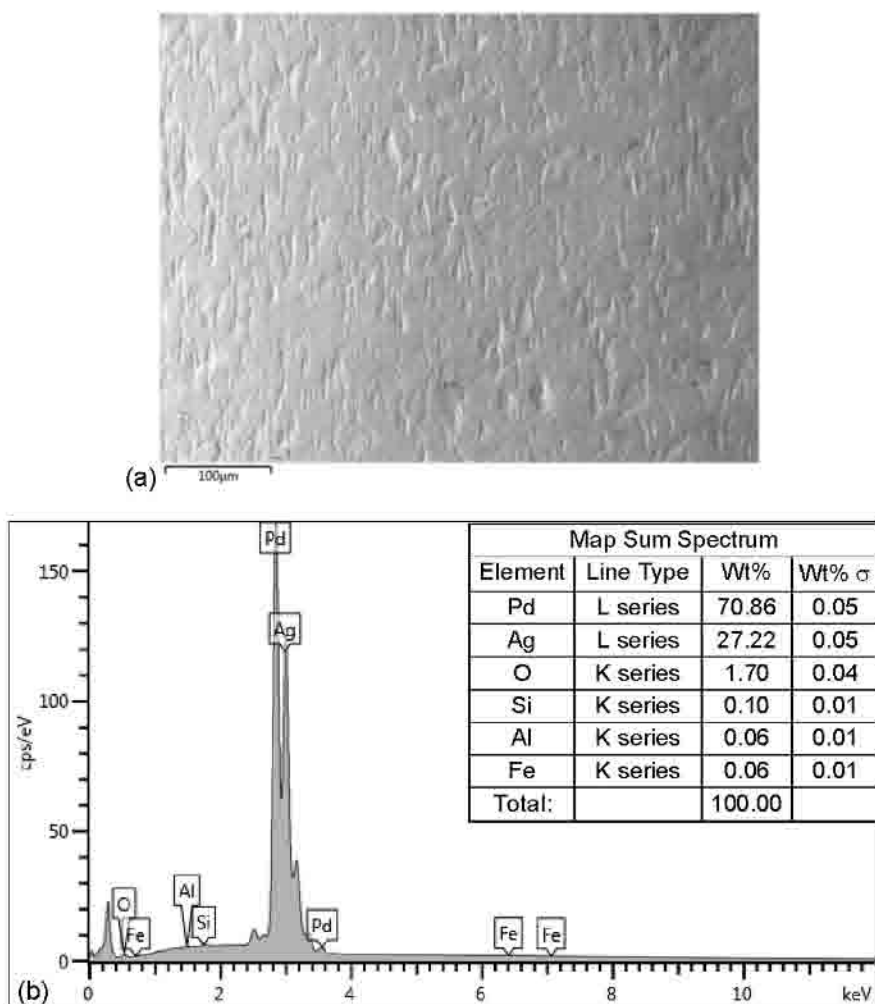


Fig. 3 (a) Pd25Ag as-received tube: control. (b) Map sum spectrum of unexposed control Pd25Ag tube with data error listed in 4th column.

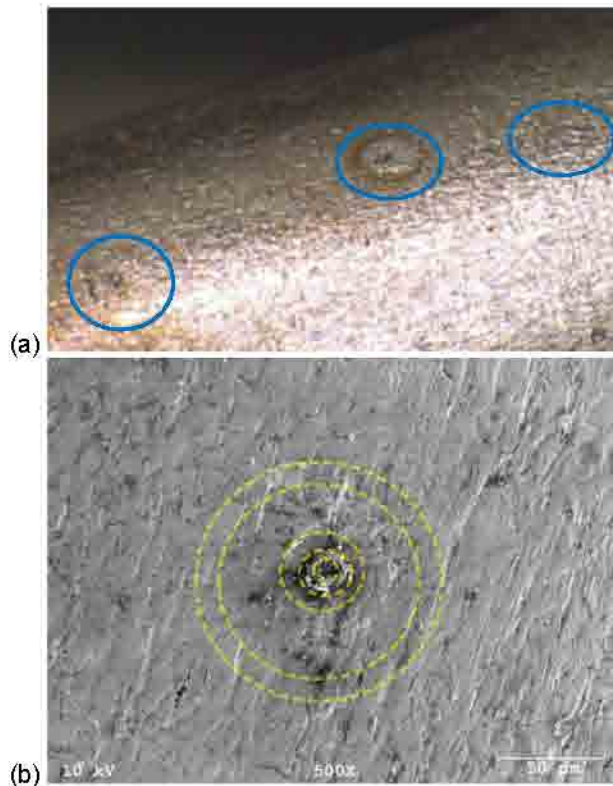


Fig. 4 Pd25Ag tube with ringed (a) and bulls-eye features (b).

the experiment. Biberian and Armanet [3] also observed molten features and surface ripples in their experiments. Furthermore, it is surmised that the features did not come from outside (i.e., a pebble dropped in water), but rather they came from inside because there was not evidence of a raised structure in the middle of the crater.

Table 2 provides the microprobe analysis of the small particle in the center of the bulls-eye feature. The analysis shows that the crater is rich in Ca, Cr, and Fe, with lesser amounts of Pd, Mn, Ti, K, Cl, S, Si, Al, Mg, Na, and O. Note that Pd is only 58.32 counts/second ± 2.37 counts/second (10.97 wt %) and Ag is 0.00 counts/sec ± 1.93 counts/sec (0.00 wt %). The data includes uncertainties of 2σ as indicated in the 'Error 2σ ' column.

Another interesting site was located on the exposed Pd25Ag tube and showed a small kidney-shaped area of Ti near the middle of the image. Fig. 5(a) shows the area of the tube.

Fig. 5(b) provides the EDS analysis of the area in the center of the kidney-shaped feature. The analysis shows that the crater is rich in Pd, O, and Ti, with lesser amounts of N, Ag, Ca, Zn, Na, Cl, Al, S, Fe, Mg, and Si. Note that the amount of Pd is only 57.55 ± 0.80 wt %, and the amount of Ag is small at 3.52 ± 0.38 wt %. This analysis suggests that a portion of the Pd and/or Ag from the tube was transmuted into other elements not present before the cycling of the deuterium gas.

Table 2 EDS analysis of small bulls-eye feature from Pd25Ag tube sample shown in Fig. 4(b) with data error shown in the 4th column.

Element	Line	Intensity (counts/second)	Error (counts/second) 2σ	Conc. wt%
O	Ka	23.73	1.088	3.451
Na	Ka	10.19	1.156	0.648
Mg	Ka	14.84	1.368	0.760
Al	Ka	64.39	2.062	3.142
Si	Ka	137.30	2.687	6.371
S	Ka	72.34	2.403	3.846
Cl	Ka	47.44	2.326	2.850
K	Ka	77.68	2.367	6.001
Ca	Ka	300.64	3.528	28.891
Ti	Ka	11.44	1.429	1.839
Cr	Ka	46.05	1.656	12.727
Mn	Ka	11.52	1.190	4.653
Fe	Ka	22.77	1.270	13.848
Pd	La	58.32	2.376	10.973
Ag	La	0.00	1.926	0.000
Total:				100.000

Analysis of exposed Pd25Ag tubes: JM-2

After opening JM-2, the Pd25Ag tubes were extracted and then prepared for material analyses as described next.

i. Inductively Coupled Plasma Atomic Emission Spectroscopy

Two samples of Pd25Ag tube were analyzed using the ICP-AES method which analyzes the whole sample in bulk. The control unexposed tube contained bulk amounts of Pd and Ag as expected with a 3:1 ratio (Table 1). In addition, trace amounts of Al, Cu, Fe, Mg, Na, Pt, and Si are present within 0.5 parts per million minimum detection. Table 1 also shows the results from an exposed Pd25Ag tube. Bulk amounts of Pd and Ag were detected as expected, but in addition there were various amounts of Cr, Cu, Fe, Mn, Si, and Zn, which are different from the amounts found in.

The unexposed Pd25Ag tube. In fact, there seems to be 7 times as much Cu and 2 times as much Fe than in the exposed sample, and new amounts of Cr, Mn, and Zn compared with those of the unexposed Pd25Ag sample. This analysis indicates that transmutations occurred within the Pd25Ag tube after being exposed to the pressure-cycled deuterium gas.

The data in Table 1 includes estimates on the uncertainty of the data. These uncertainties are not technically 95% confidence limits, which would have required running multiple true repeats and using statistics and percent relative standard deviation calculations. But the estimated uncertainty does take into account the general ICP-AES method imprecision, as well as the sensitivity of the emission lines used for each element plus baseline noise which impacts detection limits. Matrix effects from the sample major constituents are also considered.

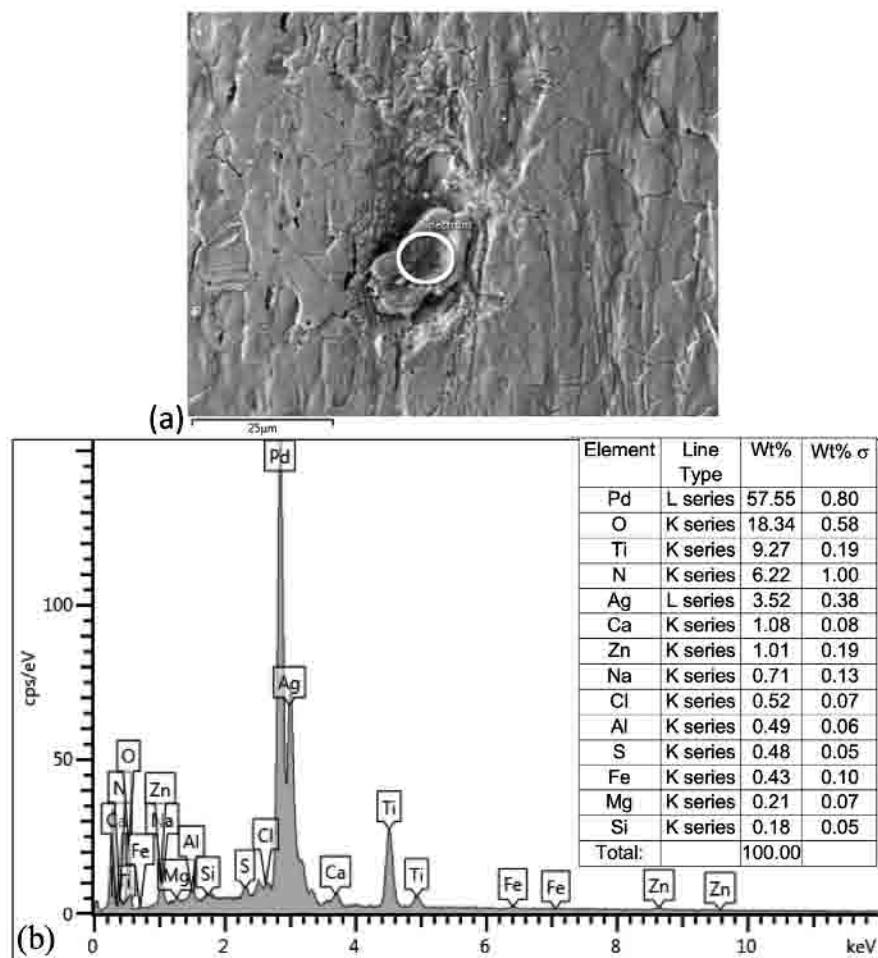


Fig. 5 SEM/EDS image of exposed Pd25Ag tube showing a kidney-shaped area of titanium (a) and EDS analysis (b).

ii. Scanning Electron Microscope Analysis

SEM/EDS of unexposed and exposed Pd25Ag tubes are shown in Figs. 6 and 7, respectively. The surface of the unexposed tube is generally uniform and shows no craters or molten-looking spots. The elemental analysis indicates that the composition of the surface examined is 72.47 ± 0.04 wt% Pd and 26.31 ± 0.03 wt% Ag at approximately an 2.67:1 ratio by weight. The balance of the surface contains O (1.06 ± 0.03 wt%) and traces of Si (0.08 ± 0.00 wt%), Fe (0.04 ± 0.01 w%), and Al (0.04 ± 0.01 wt%).

Examining the exposed Pd25Ag tube reveals a scattering of anomalies on the surface of the tube. Large areas of Cu were observed as well as an area of Zn separate from the Cu, which may indicate that no Cu–Zn alloy is present, removing the possibility of brass contamination. Another section of exposed Pd25Ag tube showed a molten-looking spot that was composed of Cu in the middle section and Zn along the outer edges of the spot. Again, the presence of the 3D molten features indicate localized heating. This analysis indicates that transmutation occurred on the surface of the Pd25Ag tube that was exposed to the deuterium gas within the JM purifier.

It is difficult to locate a Cu and Zn site on SEM/EDS and translate that same region to another analysis tool. The ability to locate specific regions is possible with focused ion beam (FIB) sectional machining, which destroys the materials as it mines the depth. A site was located on a sample, and the FIB with Ga ions was used to trench an outline estimated to be $5 \mu\text{m} \times 5 \mu\text{m}$ (width \times depth) about that site in order to locate it with both SEM/EDS and ToF-SIMS.

The spectral analysis of the section including the FIB trench was found to be Pd (62.95 ± 0.14 wt%), Ag (17.32 ± 0.12 wt%), Zn (11.20 ± 0.07 wt%), Cu (3.1 ± 0.04 wt%), and Fe (1.34 ± 0.03 wt%); and the remaining is made up of O (3.44 ± 0.12 wt%), Ni (0.53 ± 0.03 wt%), and Cr (0.13 ± 0.02 wt%). Note that the ratio between Pd and Ag is 3.51:1, which is larger than the 2.67:1 ratio of unexposed Pd25Ag. A color map of the same area is shown in Fig. 8; it shows the location of each element detected via EDS. A moderate amount of Zn appears throughout the sample, and Cu and Fe appear in several bright spots. However, focusing at high resolution on the FIB trench (with more uniform Zn distribution potentially related to softening and zinc's melting point at 420°C) shows some Ga residual from the FIB trenching with Cu and Zn along each side of the trench and a significant amount of Pd and Ag in the

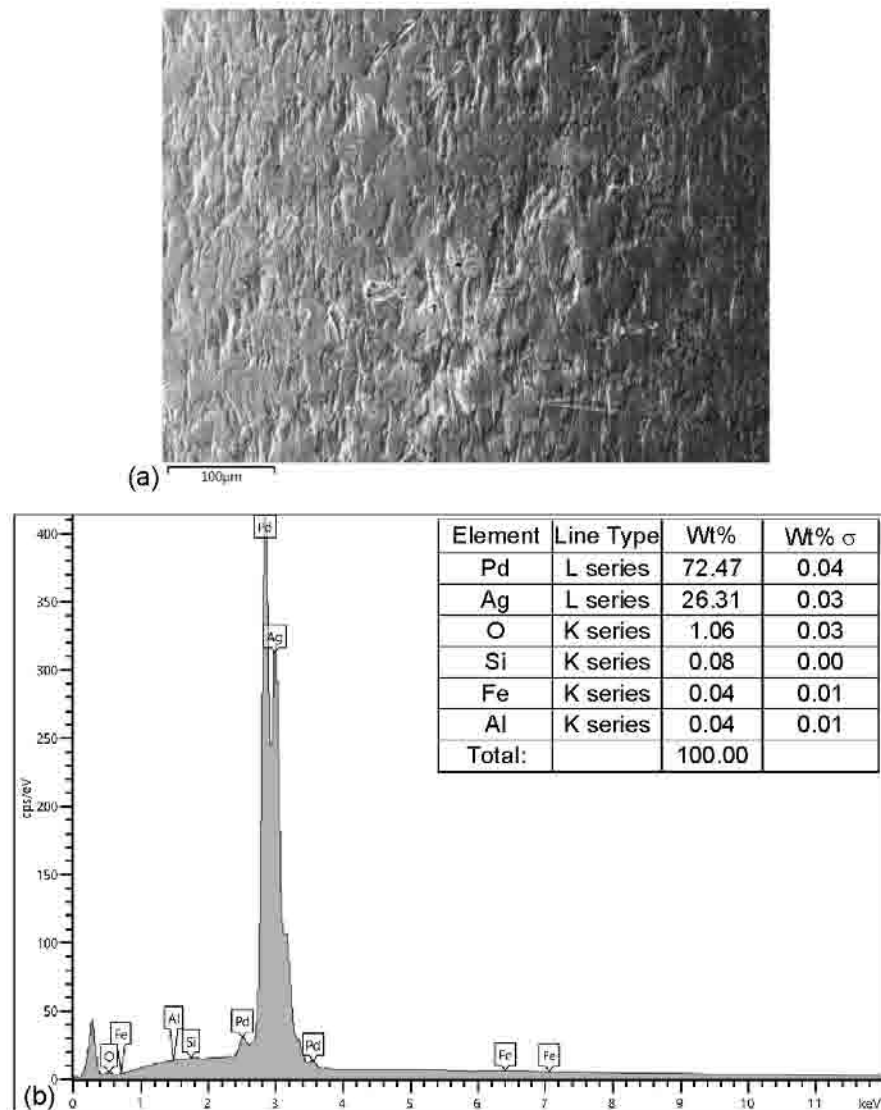


Fig. 6 SEM/EDS image of unexposed Pd25Ag tube (a) and spectral analysis (b).

trench. This observation indicates that the transmutations seen are a surface effect.

iii. Time-of-Flight Secondary Ion Mass Spectrometry

The exposed Pd25Ag tube with an FIB trench was analyzed via ToF-SIMS to gain isotopic information of the sample. The instrument used was a PHI (Physical Electronics USA) Trift V NanoTOF. The primary ion was ^{69}Ga at 30 kV, with about a 150-nm spot size. The peaks that were of most interest are listed in Table 3 and coincide with the Cu, Zn, Cr, and Fe detected in both the ICP-AES and SEM/EDS analyses. For the peaks of interest, the ToF-SIMS resolution is from 17 to 26 milli-amu. The 2σ error ranges from ± 37 to 68 counts where the signal counts range from 237,857 for ^{64}Zn counts to 5,832,543 counts for ^{56}Fe as outlined in Table 3.

The data confirm the presence of Cu, Zn, Fe, and Cr as was discovered during the ICP-AES and SEM/EDS analyses. Based on the ToF-SIMS data obtained, there are several conclusions that can be reached:

- 1) The spatial correlation between Cu and Zn is weak (Fig. 9), indicating that brass is not a source of contamination.
- 2) The spatial correlation between Fe and Cr (Fig. 10) is weak, indicating SS is not a source of contamination.
- 3) The isotopic distribution of all of the anomalous elements is within the normal range expected for natural abundance.
- 4) The spatial correlation between Pd and Ag is not as good as would be expected for a homogeneous sample of 75% Pd and 25% Ag, indicating possible transmutations.

Thus, the TOF-SIMS data is enigmatic. Some aspects favor Pd25Ag transmutation to explain the Cu, Zn, Fe, and Cr. Other

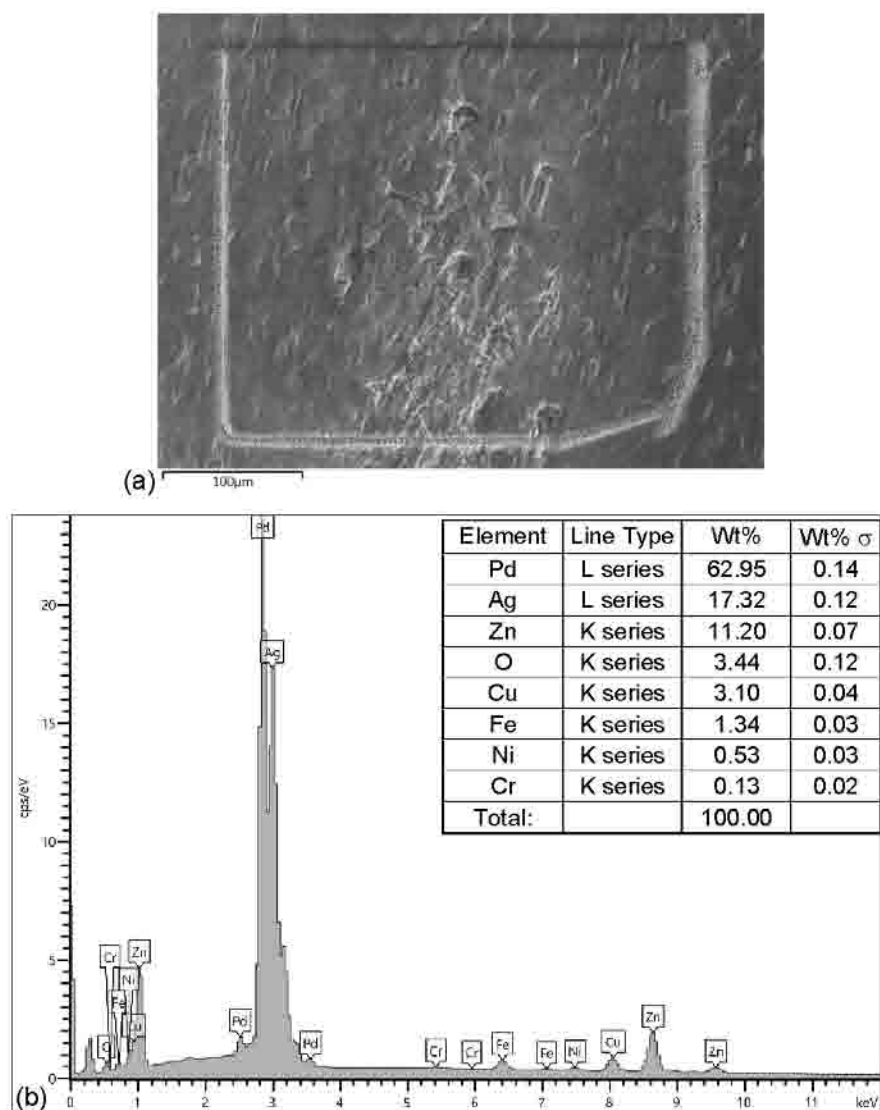


Fig. 7 SEM/EDS image of exposed Pd25Ag tube with FIB rectangular trench (a) and spectral analysis (b).

aspects of the data suggest contamination, although the Zn map pattern is not consistent with Cu diffusion from brass contamination.

The natural abundance ratio of ^{108}Pd : ^{110}Pd is nearly the same as the ^{63}Cu : ^{65}Cu ratio. Deuteron-induced Pd fission to Cu and Ar would produce the two stable Cu isotopes in nearly the exact ratio of natural abundance, along with some other unstable short-lived Cu isotopes, however other Pd isotopes (including the primary, ^{106}Pd), would only produce unstable Cu isotopes. The net result would be normal Cu isotopic distribution. The path to natural abundance is not so easy with the other anomalous elements of Zn, Fe, and Cr observed with both ToF-SIMS and SEM/EDS mapping.

Discussion of analytical results

As discussed within each section of analytical results, there seems to be evidence of material transmutations of Pd and Ag

on the surface of the Pd25Ag exposed tube. From the bulk analysis with ICP-AES indicating increased amounts of Cu and Fe, and the emergence of Cr and Zn that were not seen in the unexposed tube sample, to the SEM/EDS data indicating the presence of Cu, Fe, Cr, and Zn, to the ToF-SIMS data showing areas of Cu, Fe, Cr, and Zn; there is corroborating evidence of changes to the surface of the Pd25Ag tubes after exposure to deuterium gas.

But beyond the transmutations is there some possibility that there has been diffusion and enrichment of the metals identified from the inside towards the surface? Could we be seeing material from the SS spring inside the tube thermally diffuse and travel to the surface? Not likely since the melting points of Cu, Fe, Cr, and Zn are 1085 °C, 1538 °C, 1907 °C, and 419.5 °C respectively. All of these melting points are above the operating conditions of the experiment where the temperatures were kept under 400 °C. In addition, the means as to which this could occur indicates that Cu, Fe, Cr, and Zn from the inner SS spring wire or other contaminated areas would

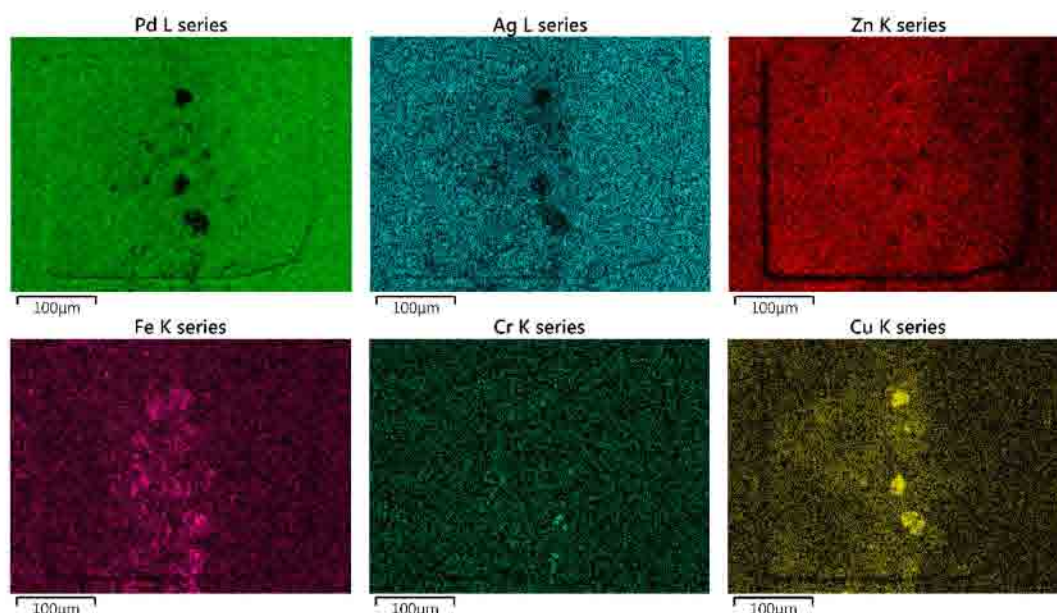


Fig. 8 SEM/EDS color maps of exposed Pd25Ag tube with an FIB trench showing Pd, Ag, Zn, Fe, Cr, and Cu. (For interpretation of the references to color in this figure legend, the reader is referred to the Web version of this article.)

Table 3 ToF-SIMS analysis showing the Cr, Fe, Cu and Zn isotopes detected in the area on the Pd25Ag tube sample shown in Fig. 7(a).

Element	Atomic Mass Unit	Counts	Background Counts	Error 2 σ	FWHM (amu)
^{64}Zn	63.93	237,857	456	42.71	0.026
^{63}Cu	62.93	786,909	339	36.82	0.020
^{52}Cr	51.94	1,204,413	486	44.09	0.017
^{56}Fe	55.94	5,832,543	1172	68.47	0.018

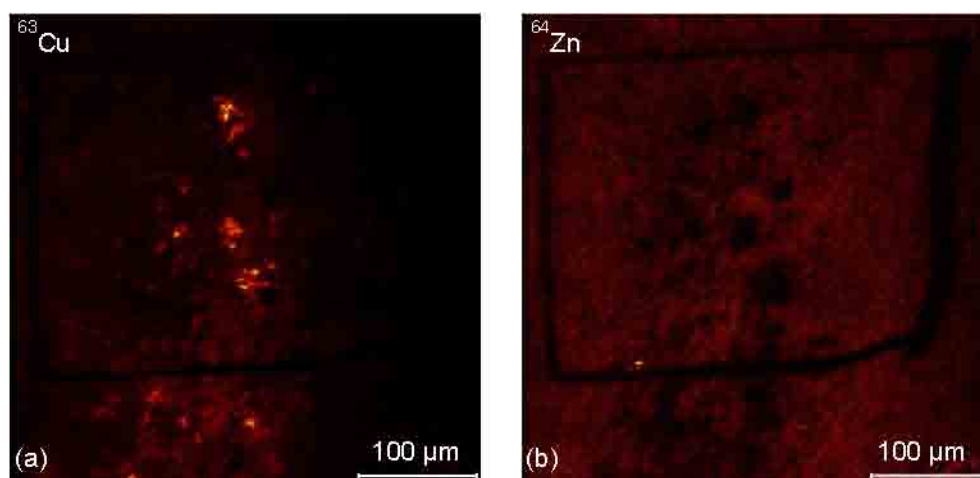


Fig. 9 ToF-SIMS analysis in and around the FIB trench showing evidence of ^{63}Cu (a) and ^{64}Zn (b).

have to transport from the inner portion of the Pd25Ag tube to the surface for a distance of 0.08 mm. Furthermore, the spatial correlations between both Cu and Zn, and Fe and Cr are weak as shown in the ToF-SIMS data. If both pairs of elements were in the same location on the Pd25Ag tube, that would indicate some kind of brass or SS contamination.

It is also noted by the SEM/EDS analysis of the JM-2 tubes that the ratio between Pd and Ag is 3.51:1 in the exposed Pd25Ag. This ratio is larger than the 2.67:1 ratio of unexposed Pd25Ag. The change in ratio indicates that either the Pd has increased from the cycling of deuterium or that the Ag has decreased from the cycling. This ratio change of the original

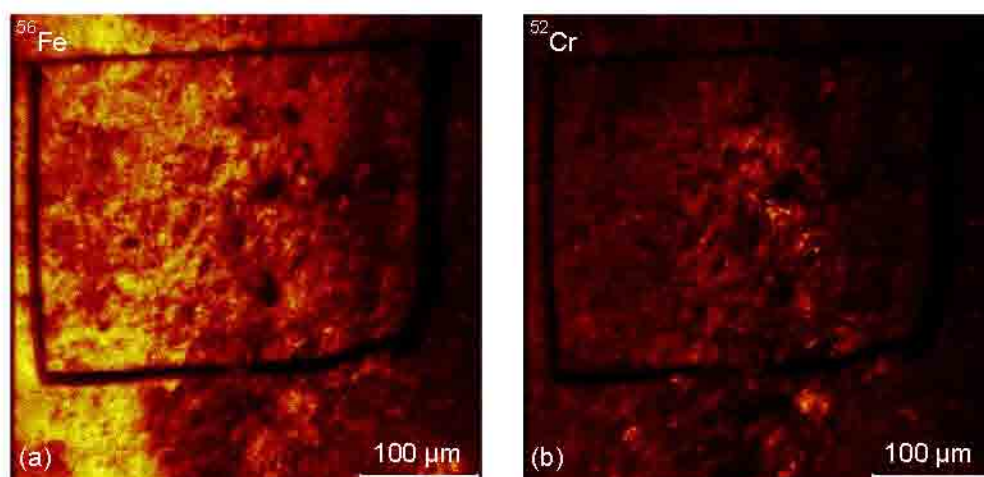


Fig. 10 ToF-SIMS analysis in and around FIB trench showing evidence of ^{56}Fe (a) and ^{52}Cr (b).

Pd and Ag elements is further evidence of material transmutation under these deuterium cycling conditions.

Conclusions

The data and results reported here illustrate that JM-1 and JM-2 testing using isotopic-hydrogen loading with pressure and thermal cycling of Pd25Ag matrix materials engenders anomalous heat and material changes, albeit at low energy. The results of the most recent JM purifier experiment (JM-2) with three coils of Pd25Ag pressure cycled with deuterium gas have been presented. The data indicate possible nuclear transmutations were found on the surface. Since transmutations release MeVs of energy, localized heating and shock propagation would be expected and account for the 3D nature of some of the features present. A future paper will address this heating process and mechanisms in more detail. The data and results reported here illustrate that JM-1 and JM-2 testing using isotopic-hydrogen loading with pressure and thermal cycling of an Pd25Ag alloy induces anomalous material changes. Independent researchers have found similar transmutations [2,11,13–18] or energetic nuclear emissions [19,20] with Pd and D under different experimental conditions.

The origin of deuterium-PdAg25 energetic sites (anomalous heating) is complicated by absorption and desorption profiles related to α phase, with occupied octahedral sites, and β phase occupying tetrahedral sites. However, Johansson [21] and Anand [22] find β phase doesn't exist in the $>300^\circ\text{C}$ JM operating temperature range. The mechanism that eliminates octahedral occupancy may also reduce the number of superabundant vacancies available to hold hydrogen isotopes. The JM gas separator is noted for efficiently separating hydrogen isotopes from other gasses and not necessarily maintaining high loading.

Johnson [23] notes nanocrystal facets, site occupancy and lattice strained vertices also govern desorption. The extrusion process used to manufacture the thin wall tubes may provide preferential grain and hence facet, orientation in the JM tubes aiding desorption. McCool and Lin [24] found that 20–60 nm

crystallite sizes increase hydrogen permeability with increasing size. However, Pd grain growth begins $>400^\circ\text{C}$. This is below the JM operating temperature and should preserve the original grain size and orientation. Rapid desorption is necessary for the hydrogen isotope flux required for the observed transmutation processes. The 50°C lower desorption temperature of deuterium vs hydrogen at 1 bar [22], may further increase deuterium flux as compared to slower hydrogen recombination.

Sufficiently strained lattice vertices [27] will drive paramagnetic Pd to be ferromagnetic. Previous work has shown that Pd lattice strain induced itinerant ferromagnetism [25] is related to transmutation. Evidence of transmutations from Pd and Ag to various elements including Cu and Zn have been observed here. Many of the possible reactions between Pd and D, and Ag and D were found to be exothermic which coincides with the observation of localized heating at the sites containing the Cu and Zn products. Although the mechanism of how these products were created is not conclusively known at this time, several possibilities include electron screening [26], deuteron capture, neutron capture, or proton capture and then subsequent nuclear disintegration or fission of the starting elements. Future tests to further reproduce the transmutations and better track the “before” and “after” states of the Pd25Ag tube are planned.

Declaration of competing interest

The authors declare that they have no known competing financial interests or personal relationships that could have appeared to influence the work reported in this paper.

Acknowledgements

The authors would like to acknowledge Dave Carr of Physical Electronics USA (PHI) for performing the ToF-SIMS analysis. Funding for this work was provided by NASA Headquarters Planetary Sciences Division Science Mission Directorate.

REFERENCES

- [1] Fralick GC, Decker AJ, Blue JW. "Results of an attempt to measure increased rates of the reaction $^2\text{D} + ^2\text{D} \rightarrow ^3\text{He} + \text{n}$ in a nonelectrochemical cold fusion experiment," NASATM-102430. 1989. <https://ntrs.nasa.gov/search?highlight=true&q=TM-102430>.
- [2] Li XZ, Liu B, Ren XZ, Tian J, Cao DX, Chen S, Pan GH. "Super-absorption" – correlation between deuterium flux and excess heat. Proceedings of the ICCF-9, Tsinghua University Press 2003:197. <https://www.lenr-canr.org/acrobat/LiXZsuperabsor.pdf>.
- [3] Biberian J-P, Armanet N. Excess heat during diffusion of deuterium through palladium. In: Proceedings of the ICCF-13, sochi, Russia; 2007. <https://www.lenr-canr.org/acrobat/BiberianJPexcessheatd.pdf>.
- [4] Liu B, Li XZ, Wei QM. 'Excess heat' induced by deuterium flux in palladium film. J. of Condensed Matter Nuclear Science 2006;75–9. https://www.worldscientific.com/doi/abs/10.1142/9789812772985_0007.
- [5] Ackerman FJ, Koskinas GJ. Permeation of hydrogen and deuterium through palladium-silver alloys. J Chem Eng Data 1972;17:51–5. <https://pubs.acs.org/doi/pdf/10.1021/je6052a011>.
- [6] Vadrucchi M, Borgognoni F, Moriani A, Santucci A, Tosti S. Hydrogen permeation through PdAg membranes: surface effects and Sieverts' Law. Int J Hydrogen Energy 2013;38:4144–52. <https://www.sciencedirect.com/science/article/abs/pii/S0360319913002000>.
- [7] Smith PJ. Permeation rate equations for hydrogen and deuterium in a palladium-silver alloy. 2019. NASATM-2019-220189, <https://ntrs.nasa.gov/citations/20190030498>.
- [8] Tosti S, Adrover A, Basile A, Camilli V, Chiapetta G, Violante V. Characterization of thin wall Pd-Ag rolled membranes. Int J Hydrogen Energy 2003;28:105–12. <https://www.sciencedirect.com/science/article/abs/pii/S0360319902000344>.
- [9] Tagliabue M, Delnero G. Optimization of a hydrogen purification system. Int J Hydrogen Energy 2008;33:3496–8. <https://www.sciencedirect.com/science/article/abs/pii/S0360319908004837>.
- [10] Storms E. The science of low energy nuclear reaction. World Scientific Publishing; 2007. 13: 978-9812706201.
- [11] Liu B, Dong ZM, Liang CL, Li XZ. Nuclear transmutation on a thin Pd film in a gas-loading D/Pd system. J. of Condensed Matter Nuclear Science 2014;13:311–8. <https://www.lenr-canr.org/acrobat/BiberianJPcondensedl.pdf#page=321>.
- [12] Miley GH, Hora H, Yang X. Condensed matter "cluster" reactions in LENRs. Proceedings of the ICCF-14, Washington, DC 2008. <https://www.lenr-canr.org/acrobat/MileyGHcondensedm.pdf>.
- [13] Iwamura Y, Itoh T, Gotoh N, Toyoda I. Detection of anomalous elements, x-ray and excess heat in a D₂-Pd system and its interpretation by the electron-induced nuclear reaction model. Fusion Technol 1998;33(4):476–92. <https://www.tandfonline.com/doi/abs/10.13182/FST98-A47>.
- [14] Iwamura Y, Itoh T, Tsuruga S. Increase of reaction products in deuterium permeation-induced transmutation. J. of Condensed Matter Nuclear Science 2014;13:242–52. <https://www.lenr-canr.org/acrobat/BiberianJPcondensedl.pdf#page=252>.
- [15] Iwamura Y, Itoh T, Yamazaki N, Kasagi J, Terada Y, Ishikawa T, Sekiba D, Yonemura H, Fukutani K. Observation of low energy nuclear transmutation reactions induced by deuterium permeation through multilayer Pd and CaO thin film. J. of Condensed Matter Nuclear Science 2011;4:132–44. <https://www.lenr-canr.org/acrobat/BiberianJPcondensedc.pdf#page=140>.
- [16] Kitamura A, Takahashi A, Takahashi K, Seto R, Hatano T, Iwamura Y, Itoh T, Kasagi J, Nakamura M, Uchimura M, Takahashi H, Sumitomo S, Hioki T, Motohiro T, Furuyama Y, Kishida M, Matsune H. Excess heat evolution from nanocomposite samples under exposure to hydrogen isotope gases. Int J Hydrogen Energy 2018;43:16187–200. <https://www.sciencedirect.com/science/article/pii/S0360319918320925>.
- [17] Takahasi A, Ohta M, Mizuno T. Production of stable isotopes by selective channel photofission of Pd. Jpn J Appl Phys 2001;40:7031–46. <https://iopscience.iop.org/article/10.1143/JJAP.40.7031/pdf>.
- [18] Szpak S, Mosier-Boss PA, Young C, Gordon FE. Evidence of nuclear reactions in the Pd lattice. Naturwissenschaften 2005;92:394–7. <http://link.springer.com/article/10.1007/s00114-005-0008-7>.
- [19] Schenkel T, Persaud A, Wang H, Seidl PA, MacFadyen R, Nelson C, Waldron WL, Vay J-L, Deblonde G, Wen B, Chiang Y-M, MacLeod BP, Ji Q. Investigation of light ion fusion reactions with plasma discharges. J Appl Phys 2019;126:203302. <https://doi.org/10.1063/1.5109445>.
- [20] Jorne J. Neutron and gamma-ray emission from palladium deuteride under supercritical conditions. Fusion Technol 1991;19(2):371–4. <https://doi.org/10.13182/FST91-A29371>.
- [21] Johansson M, Skulason E, Nielsen G, Murphy S, Nielsen RM, Chorkendorff I. Hydrogen adsorption on palladium and palladium hydride at 1 bar. Surf Sci 2010;604:718–29. <https://www.sciencedirect.com/science/article/abs/pii/S0039602810000385>.
- [22] Anand NS, Pati S, Jat RA, Parida SC, Mukerjee SK. Thermodynamics and kinetics of hydrogen/deuterium absorption-desorption in Pd_{0.77}Ag_{0.23} Alloy. Int J Hydrogen Energy 2015;40:444–50. <https://www.sciencedirect.com/science/article/pii/S0360319914029759>.
- [23] Johnson NJ, Lam B, MacLeod BP, Sherbo RS, Moreno-Gonzalez M, Fork DK, Berlinguette CP. Facets and vertices regulate hydrogen uptake and release in palladium nanocrystals. Nat Mater May 2019;18:454–8. <https://doi.org/10.1038/s41563-019-0308-5>.
- [24] McCool BA, Lin YS. Nanostructured thin palladium-silver membranes: effects of grain size on gas permeation properties. J Mater Sci 2001;36:3221–7. <https://link.springer.com/content/pdf/10.1023/A:1017938403725.pdf>.
- [25] Mosier-Boss PA, Forsley LPG, McDaniel PK. Investigation of nano-nuclear reactions in condensed matter: final report. DTRA 2020:75–7. <https://doi.org/10.13140/RG.2.2.31859.53282>.
- [26] Pines V, Pines M, Chait A, Steinetz BM, Forsley L, Hendricks RC, Fralick GC, Benyo TL, Baramsai B, Ugorowski PB, Becks MD, Martin RE, Penney N, Sandifer II CE. Nuclear fusion reactions in deuterated materials. Phys Rev C 2020;101:044609. <https://journals.aps.org/prc/abstract/10.1103/PhysRevC.101.044609>.
- [27] Dechiaro L, Forsley LPG, Mosier-Boss PA. Strained layer ferromagnetism transition metals and its impact upon low energy nuclear reactions. J Condens Matter Nucl Sci 2015;17:1–26. In press, <https://www.lenr-canr.org/acrobat/BiberianJPcondensedp.pdf#page=6>. [Accessed 24 September 2020].